



## Electroless and Corrosion of Nickel-Phosphorus-Tungsten Alloy

M.S. Ali Eltoum

Department of Chemistry, Faculty of Science, Sudan University of Science and Technology, Khartoum, Sudan  
[abotrteell74@gmail.com](mailto:abotrteell74@gmail.com)

**Abstract:** At the present work Nickel-Phosphorous- tungsten alloy was electroless plating on copper substrate, different parameters which affect the electroless plating of this alloy were studied and the obtained coatings were characterized using different analytical techniques such as EDX (Energy Dispersive X-ray), XRD (X-ray Diffraction), SEM (Scanning Electron microscope), Potentiodynamic polarization curve (corrosion resistance), incorporation of tungsten on Ni-P matrix changed the crystallography and microstructure details of Ni-P ally and enhancement in corrosion and hardness were observed.

### To cite this article

[Ali Eltoum, M. S. (2016). Electroless and Corrosion of Nickel-Phosphorus-Tungsten Alloy. *J. Middle East North Afr. sci.*, 2(2), 16-24]. (p-ISSN 2412- 9763) - (e-ISSN 2412-8937). <http://www.jomenas.org>. 2

**Keywords:** Electrolessplting; Polyalloy; Potentiodynamic polarization; Corrosion.

### 1. Introduction

Development of electroless nickel polyalloy deposits is considered as the most effective method to alter the chemical and physical properties of binary Ni-P alloy deposits. The transition metal is the preferred choice because of its high melting temperature, and, unusual mechanical properties.

It is a well-established fact that W cannot be electrodeposited from aqueous electrolytes, but can be codeposited with iron group metals such as nickel to form an alloy (Brenner, 1963), this is classified as induced codeposition.

Electroless ternary alloy with elements other than the iron family, namely, Ni-W-P, has been first reported by Pearlstein, Weightman, and Wick (1963). Codeposition of tungsten in binary Electroless Ni-P deposit improves the deposit characteristics such as wear resistance. The properties of the electroless Ni-W-P amorphous deposits were determined (Bangewi, Wangyu, Qinglong, & Xuanyuan, 1996). Ni-P based alloy films was prepared by autocatalytic plating and their structure, chemistry and corrosion behaviors in sulfuric acid solution were studied as a function of their composition (Lu & Zangari, 2002). The as-prepared Ni-based alloys are nanocrystalline, and their grain size decreases with increasing P content. The Addition of a third element (W or Mo) influences the observed grain size.

Electroless deposition of Ni-W-P alloy coatings onto metal substrates using H<sub>2</sub>PO<sub>2</sub> as reducing agent from solutions containing nickel sulfate, sodium tungstate, sodium citrate, ammonium sulfate and other additives was studied (Du & Pritzker, 2003). Electroless Ni-P-W coatings were deposited on mild steel in alkaline solutions have been reported (Tien, Duh, & Chen, 2004). The tungsten addition into the nickel-phosphorus based coating, effectively, increases micro hardness and thermal stability (Balaraju & Rajam, 2005). They also possess good magnetic properties. The effect of copper and tungsten in alkaline electroless nickel baths has been studied in depositing Ni-Cu-P and Ni-W-P alloys and also the synergistic effect of ions in depositing Ni-W-Cu-P alloys (Balaraju & Rajam, 2005). Autocatalytic ternary Ni-Sn-P, Ni-W-P and quaternary Ni-W-Sn-P films were also studied (Balaraju & Rajam, 2006). Alkaline citrate-based baths were used and compared with binary Ni-P coatings, excellent properties such as high hardness, wear and corrosion resistance, a lot of interest has been created in the scientific community in developing electroless nickel alloys Hypophosphite reduced baths become more popular for many industrial applications due to their stability, ease of operation, and cost effectiveness.

Thermal stability of electroless Ni-W-P deposits, analyzed by DSC, is enhanced by the co-deposition of tungsten as compared to binary electroless Ni-P coating (Hu, Wang, Meng, & Rao, 2006). Quaternary Ni-W-Cu-P coatings deposited using alkaline-citrate-based nickel sulfate and nickel chloride baths were studied (Balaraju, Anandan, & Rajam, 2006). Incorporation of copper has a marginal influence on the nickel, phosphorus and tungsten contents of the coatings. XPS studies show that the addition of copper increases the elemental form of W in chloride-based deposits towards that of sulfate-based deposits. Copper has no detrimental effect on hardness, but improves the surface quality difference in hardness between ternary and quaternary deposits.

Composite four-component Ni-W-P-ZrO<sub>2</sub> coatings were electrolessly deposited from a bath with different concentrations of glycine, sodium tungstate (VI) and zirconium (IV) oxide at different pH values (Szczygieł & Turkiewicz, 2008).

The effect of experimental parameters, such as temperature, pH, nickel sulfate concentration, sodium hypophosphite concentration, sodium citrate concentration, and deposition time on the deposition rate of electroless deposition of Ni-P-W and Ni-P-Al<sub>2</sub>O<sub>3</sub> were studied (Hamdy, Shoeib, Hady, & Salam, 2008). The result shown that, the coating brightness, coherence, corrosion and uniform surface distribution were improved due to addition of W and alumina. Ni-W-Cr-P alloy coatings prepared by electroless deposition on stainless steel have been reported by Jin et al. (2010). The effects of heat treatment on the structure and phase transformation behavior, microhardness of the Ni-W-Cr-P alloy coatings were investigated. The experimental results reveal that with an increase in the annealing temperature, micro hardness of Ni-W-Cr-P alloy coatings increased, reaching its maximum value at 700C, and then decreased slightly. Using a complexing agent such as citrate in electroless Ni-P such as citrate (Hamdy, Shoeib, Hady, & Salam, 2008), propylene glycol and urea (de Hazan, Werner, Z'graggen, Groteklaes, & Graule, 2008) are found to induce stability during plating. A survey of the literature shows that gluconate electrolytes have been used to electroplate metals such as nickel (Abd El Meguid, Abd El Rehim, & Moustafa, 1999), copper (El Rehim, Sayyah, & El Deeb, 2000), tin (Abd el Rehim, Sayyah, & El Deeb, 2000), and zinc (Rashwan, Mohammed, El Wahaab, & Kamel, 2000). No literature reference was found on the use of gluconate in electroless nickel plating. The objective of the present study is to obtain Ni-P-W from alkaline gluconate baths, studying the dependence of coating characteristics on several

electroless plating variables. Our work also characterizes the coatings by using different analytical techniques such as SEM, EDX and XRD and examines the coating hardness and corrosion resistance.

## 2. Experimental

### 2.1. Chemicals of electroless deposition:

All chemicals used were of analytical grade: Nickel sulfate hexa-hydrate (NiSO<sub>4</sub>.6H<sub>2</sub>O), Boric acid (H<sub>3</sub>BO<sub>3</sub>), Ammonium sulfate ((NH<sub>4</sub>)<sub>2</sub>SO<sub>4</sub>), Sodium gluconate (C<sub>6</sub>H<sub>11</sub>O<sub>7</sub>Na), Sodium tungstate (Na<sub>2</sub>WO<sub>4</sub>), Sodium hydroxide (NaOH), Sodium carbonate (Na<sub>2</sub>CO<sub>3</sub>), Hydrochloric acid (HCl), Sulfuric acid (H<sub>2</sub>SO<sub>4</sub>), Nitric acid (HNO<sub>3</sub>), Acetone (C<sub>2</sub>H<sub>6</sub>O), Ethanol (C<sub>2</sub>H<sub>6</sub>O), Sodium hypophosphite (NaH<sub>2</sub>PO<sub>2</sub>), lead acetate (PbAc<sub>2</sub>), Succinic acid (C<sub>4</sub>H<sub>6</sub>O<sub>4</sub>), (Sodium dodecyl sulfate (SDS), (C<sub>12</sub>H<sub>23</sub>O<sub>4</sub>SNa), Palladium chloride (PdCl<sub>2</sub>).

### 2.2. Pretreatment of the substrates:

Before each run, the copper sheets cathodes (2X2cm<sup>2</sup>) were mechanically polished with different grades emery papers (360,800 and 1000) and then washed by distilled water, then degreased by ethanol (abs 95%) for 60 second, rinsed by distilled water, pickled by acidic solution (3HCl+1HNO<sub>3</sub>), for 30 second, rinsed by distilled water, anodically polarized in concentrated Phosphoric acid for 2min at 4V for electro-polishing and rinsed by distilled water, the copper sheets were then dried with hot air to be ready for the electroplating process.

### 2.3. Activation of copper substrate:

After treating the copper substrate, it was immersed for 20 seconds in a dilute acidic solution of PdCl<sub>2</sub> (0.1 g/L PdCl<sub>2</sub> and 0.2 ml/L HCl 36%), followed by thorough rinsing, then the substrate was dried and weighed (9).

### 2.4. Experimental procedure of nickel electroless deposition:

The electrochemical cell was connected by holding only the copper substrate immersed into 250ml of the electroless solution for 60 min.

#### 2.4.1. Bath composition of Nickel-phosphorus electrolessdeposition:

The plating bath composition and operating condition are shown in Table (1) below:

Table 1: *The plating bath composition and operating condition.*

Nickel sulfate	5-30 g/L
Sodium hypophosphite	5-40 g/L
Sodium gluconate	15-40 g/L
Succinic acid	3 g/L
SDS	0.5g/L
Lead acetate	2 mg/L
Time	20-100 min
Temperature	50-100 <sup>0</sup> C
pH	4-9
Stirring speed	150 rpm

The pH was measured using Microprocessor pH/mV/C Meter (Model CP 5943-45USA) and adjusted by adding NH<sub>4</sub>OH or H<sub>2</sub>SO<sub>4</sub> 20 % solutions; the temperature was adjusted using a thermostatically controlled bath.

#### 2.4.2. Factors Affecting Electroless Ni-P alloy Coating:

The factors may be summarized as follows:

- (I). Base metal: Good quality base metal produces good quality electroless nickel coatings.
- (II). Pretreatment and cleaning: The substrate surface must be prepared to leave a clean, uniformly active, surface, and free from dirt and grease.
- (III). Electroless nickel process control; The process parameters are: Bath temperature, Bath pH, Nickel content, Reducing agent content, Complexing agent, and Deposition time

##### 2.4.2.1. Effect of Temperature on Deposition Rate:

The effect of electroless nickel bath temperature was determined as a function of deposition rate (mg/cm<sup>2</sup>.hr). The temperature was changed from 50-100C.

##### 2.4.2.2. Effect of pH:

The effect of pH on the deposition rate and phosphorus content was determined by changing the pH as a function of deposition rate and phosphorus content.

##### 2.4.2.3. Effect of Nickel Salt (source of nickel ions):

Using the operating conditions in Table (1) nickel sulfate concentration was changed from 5-30 g/L as a function of deposition rate.

##### 2.4.2.4. Effect of Sodium Hypophosphite (reducing agent):

The plating bath was prepared as in Table (1); the sodium hypophosphite concentration was changed from 5-40 g/L as a function of deposition rate and phosphorus content.

##### 2.4.2.5. Effect of Sodium gluconate (complexing agent):

Copper cathode prepared and plated using the optimum bath solution, shown in Table (1) the gluconate concentration was changed from 15-40 g/L as a function of deposition rate.

##### 2.4.2.6. Effect of plating time on the deposition rate:

The effect of time on the deposition rate was studied by changing the plating time from 20 to 100 min as a function of deposition rate.

#### 2.5. Factors Affecting Electroless Ni-P-W alloy:

##### 2.5.1. Bath composition of Ni-P-W electroless deposition:

The plating bath composition and operating conditions for Ni-P-W electroless deposition are shown in Table (2) below:

Table 2: *The plating bath composition and operating conditions for Ni-P-W electroless deposition*

Nickel sulfate	25 g/L
Sodium hypophosphite	15 g/L
Sodium gluconate	15 g/L
Ammonium sulfate	15 g/L
Sodium tungstate	5-25 g/L
Succinic acid	3 g/L
SDS	0.5g/L
Lead acetate	2 mg/L
Time	60 min
Temperature	900 C
pH	9
Stirring speed	150 rpm

#### 2.6. Characterization of nickel alloys electroless deposits:

##### 2.6.1. Coating investigation:

###### 2.6.1.1. Coating chemical composition:

The composition was examined using the following procedures:

- 1) The coating layer is stripped using 10% H<sub>2</sub>SO<sub>4</sub> solution. The object is then placed as an anode in an electroplating cell. The coating layer was dissolved in solution, diluted to 250 ml with bi-distilled water.
- 2) Analysis using Atomic absorption Spectrophotometer (Perkin Elymer3100, Germany).
- 3) The solution obtained is further diluted by dissolving 5ml in bi- distilled water to 250ml.
- 4) Nickel standard solutions for the elements to be detected were prepared (1g Ni metal in (1+1) HNO<sub>3</sub>. Diluted to 1 L with 1 % (v/v) HNO<sub>3</sub>), Ni- Hollow Cathode lamp, Air-Acetylene flame gases, wave length of 232 n

The results are confirmed in some samples with EDX analysis.

### 2.7. Coating Thickness:

Coating Thickness obtained was measured by taking a cross section of the coated layer using a coating thickness /Neophot2-Optical microscope (Germany).

### 2.8. Microstructure Characterization:

Metallographic examinations were carried out on the material under consideration, to correlate the parameters affecting mechanical properties, such as grain size and the distribution of the particles in the matrix, as well as the main phases and intermetallic phases present.

#### 2.8.1. Scanning Electron Microscopy (SEM) and Energy Dispersive X-ray (EDX):

Microstructures of different deposits were characterized by scanning electron microscopy (SEM), and Energy Dispersive X-ray Spectroscopy (EDXS).

The specimens were coated with golden solution and were taken at room temperature by inserting the samples through the sample holder into the inside of the instrument; Photomicrographs at different zones and magnifications were taken for each specimen at 30 kV, and was used to define the distribution of the particles in the matrix and on the grain boundaries. Photomicrographs of Energy dispersive X-ray spectroscopy (EDXS) at 10 kV was also used to determine the distribution of elements in the particles that are present in the matrix and on grain boundaries.

#### 2.8.2. X- Ray Diffraction (XRD):

XRD was performed in order to determine the constituent phases of surface and phase changes of different coated substrates. Using an X-Ray Diffractometer (Broker AXS-D8 X-ray diffractometer, ADVANCE, Germany), with a copper target ( $\text{Cu}\lambda = 1.54060\text{\AA}$ ) and Nickel filter. Selected samples of each group were recorded; Data of XRD were based on Bragg's Equation:

$$(1) \quad n\lambda = 2d\sin\theta$$

Where  $n$  = Integral number,  $\lambda$  = Wave length,  $d$  = Interplanar space, and  $\theta$  = Diffraction angle.

#### Crystallinity determination:

The average crystal size of the phases in the coating was calculated using *Debye-Scherer* formula:

$$(2) \quad D = k\lambda / B \cos\theta$$

Where  $D$  = crystal size nm,  $K = 0.8$ -- $1.3$  (usually close to unity e.g.0.9),  $\lambda$  is the wave length of the radiation  $\lambda_{\text{Cu}} = 1.54056 \text{\AA}$ ,  $B$  is the full width at half maximum, and  $\theta$  is the position of the maximum of diffraction.

The numerical procedures were facilitated with the use of computer software (PSI-Plot, poly software international, salt lake, UK).

#### 2.9. Hardness measurements:

The Vickers microhardness of deposits was measured under 50 gm. The load microhardness of the specimen material using a Shimdzu Hardness tester. The diamond is pressed into the surface of the specimen material at 50 gm load. For 15 s (the diamond produces a square indentation and an average is taken of the diagonal lengths) which is measured using a microscope and an average of triplet readings was recorded.

#### 2.10. Corrosion Resistance:

##### 2.10.1. Polarization Tests:

Electrochemical experiments were performed using A VOLTA LAB 40 (Model PGZ301) with the aid of commercial software (Volta Master 4 version 7.08). A saturated calomel electrode (SCE) and a platinumized platinum black were used as reference and auxiliary electrodes respectively, with the plated substrate as a working electrode. The electrochemical cell was filled with 3.5% NaCl.

Linear polarization technique was carried out by subjecting the working electrode to a potential range of 205 mV below and above corrosion potential ( $E_{\text{corr}}$ ) at a scan rate of 5 mV/Sec., corrosion rate was evaluated from the polarization curves by Tafel extrapolation with the aid of the commercial software (Volta Master 4 version 7.08).

Volta Master 4 calculates and displays the corrosion rate as Corr. in the  $\mu\text{m}/\text{year}$ : this rate is calculated from the corrosion current density found  $i_{\text{corr}}$ , the density,  $D$ , and the atomic mass,  $M$ , and valence,  $V$ , entered in the Tafel dialogue box. The calculation is performed as follows:

$$(3) \quad \text{Corr.rate } (\mu\text{m}/\text{year}) = \frac{i_{\text{corr.}} (\text{A}/\text{cm}^2) \times M (\text{g})}{D (\text{g}/\text{cm}^3) \times V} \times 3270$$

With:  $3270 = 0.01 \times [1 \text{ year (in seconds) } / 96497.8]$  and  $96497.8 = 1 \text{ Faraday in Coulombs.}$

### 3. Results and Discussion

#### 3.1. Ni-P alloy electrolessdeposition:

From data in table (1) systematic studies were carried out to investigate the appropriate conditions for Ni-P electroless plating, and this step was done only in the way that these conditions can be used in Ni-P-W alloy electroless plating and not discussed further here.

The obtained optimum conditions of Ni-P electroless plating were shown on the table (3).

Table 3: optimum conditions of Ni-P electroless plating

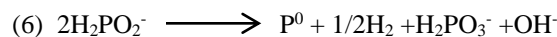
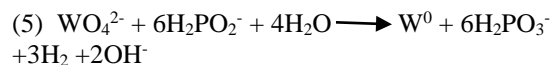
Nickel sulfate	25 g/L
Sodium hypophosphite	15 g/L
Sodium gluconate	15 g/L
Ammonium sulfate	15 g/L
Succinic acid	3 g/L
SDS	0.5g/L
Lead acetate	2 mg/L
Time	60 min
Temperature	90 <sup>0</sup> C
pH	9
Stirring speed	150 rpm

#### 3.2. Ni-P-W alloy electrolessdeposition:

##### 3.2.1. Effect of Sodium Tungstate concentration on Ni-P-W alloy:

Figs (1, 2) show the effect of sodium tungstate concentration on the deposition rate and W% in Ni-P-W alloy. The deposition rate is slightly decreased with increasing sodium tungstate concentration in the plating bath, consequently the alloy tungstate content increased and nickel content decreased. The phosphorus content slightly decreased with increase sodium tungstate concentration. This is due to increase of the metals ion ratio to hypophosphite ions in the bath. Du and Pritzker (2003), reported that Ni<sup>2+</sup> ions participate in W and P deposition, H<sub>2</sub> evolution and H<sub>2</sub>PO<sub>2</sub><sup>-</sup> oxidation and that H<sub>2</sub>PO<sub>2</sub><sup>-</sup> ions participate in cathodic reduction. This indicates that the partial reactions for the Ni-W-P system do not occur independently of one another. Finally, they proposed a mechanism for the deposition of Ni-P-W alloy that incorporates the following features: (i) produced H<sub>2</sub> originates primarily from the hypophosphite reducing agent rather than H<sub>2</sub>O and (ii) oxidation and reduction reactions mediated by radicals play very important roles in addition to anodic and cathodic processes involving direct electron transfer. These characteristics ensure that metal deposition is always accompanied by H<sub>2</sub> evolution. With this in mind, one might expect the predominant overall reactions during Ni-W-P

electroless plating in an alkaline solution to be the following:



These reactions reflect the overall stoichiometry of the processes, but not the possible mechanistic steps or interactions between the various reactants.

From Fig (3), it is clear that the deposition rate of Ni-P-W alloy increased with increasing the pH of the solution. This could be attributed to the increase of the driving force of the reducing agent as a result of the increase of which needs the addition of ammonia solution, which is a type of ligand able to enhance electron transmission, thus increasing reducing the rate of metal ions when it is incorporated with complexing agent.

The result of energy dispersive X-ray for Ni-P and Ni91%-P3%-W6% alloys were shown in Figs (4, 5) respectively.

The X-ray diffraction pattern of the as-plated Ni-W-P deposit is illustrated in Fig (7). The reflections corresponding to the (111), (200) and (220) planes of a Face Centered Cubic (FCC) phase of nickel could be observed and it was consisted of a mixture of amorphous, Ni and Ni<sub>3</sub>P. The original amorphous structure of Ni-P which has a single peak at about 42 Fig (6) was converted. This result agreed with the results obtained by Jin et.al (2010) and Aal, El-Sheikh, and Ahmed (2009). The grain size was 55.75nm.

#### 3.3. Characterization of Ni-P-W alloy:

##### 3.3.1. Morphology of Ni-P-W alloy:

The original amorphous structure of Ni-P alloy Fig (8) was converted to a compact structure with spherical nodules in the case of the morphological structure of Ni91%-P3%-W6% alloy Fig (9). Bright and coherent coatings, uniform in appearance.

##### 3.3.2. Microhardness:

The microhardness of Ni91%-P3%-W6% (W 5g/L), was observed to be 650HV50.

##### 3.3.3. Corrosion behavior Ni-P-W alloy:

The Potentiodynamic polarization curve of Ni-P and Ni-P-W coatings were shown in Figs (10,

11) respectively, and Ni-P-W has higher corrosion resistance in comparison with Ni-P. The potentiodynamic curves shown that, the corrosion current density of the coated Ni-P-W% alloy was lower than that of the Ni-p alloy. For the two curves, once the scanned potential exceeded  $E_{corr}$ , the corrosion current density of the samples continually increased. However, the increase of the corrosion current density of the coated Ni-P-W alloy was less than that of the Ni-P alloy. This implied that the anodic dissolution reaction of the Ni-W-Al<sub>2</sub>O<sub>3</sub> coating was restrained, which effectively decreased the corrosion sensitivity of the coated sample in NaCl solution.

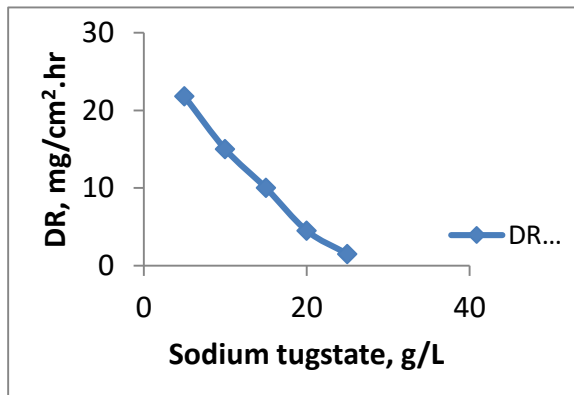


**Figure 1.** Effect of sodium tungstate g/L on DR from a bath containing NiSO<sub>4</sub>.6H<sub>2</sub>O 25g/L, Sodium hypophosphite 15g/L, Am. Sulfate 15 g/L, sodium dodecyl sulfate 0.1g/L, Succinic acid 0.3g/L, Sodium gluconate 15g/L, time 60 min, pH 9, temperature 900C.

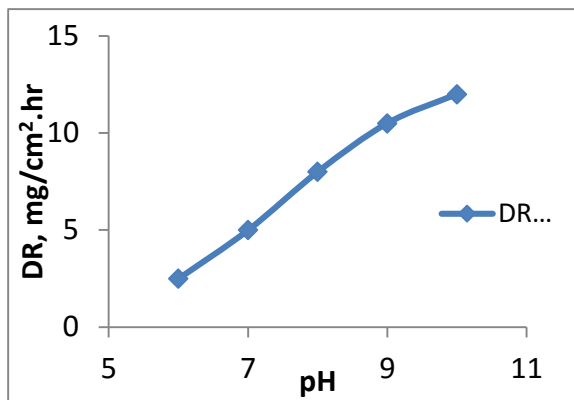


**Figure 2.** Effect of pH in the DR of Ni-P-W alloy from a bath containing NiSO<sub>4</sub>.6H<sub>2</sub>O 25g/L, Sodium hypophosphite 15g/L, sodium tungstate 15g/L, Am. Sulfate 15 g/l, sodium dodecyl sulfate 0.1g/L, Succinic acid 0.3g/L, Sodium gluconate 15g/L, time 60 min, temperature 900C.

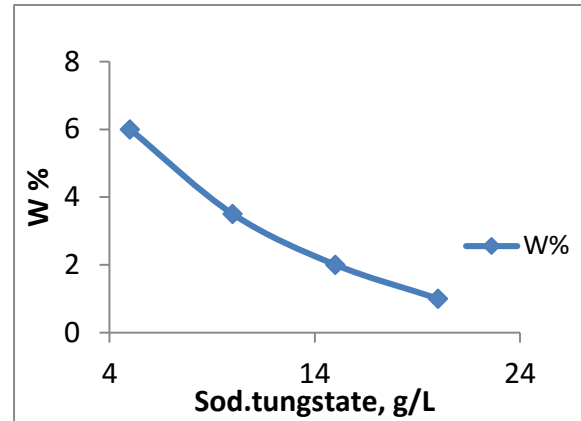


**Figure 3.** Effect of sodium tungstate g/L in W% in Ni-P-W alloy from a bath containing NiSO<sub>4</sub>.6H<sub>2</sub>O 25g/L, Sodium hypophosphite 15g/L, Am. Sulfate 15 g/L, sodium dodecyl sulfate 0.1g/L, Succinic acid 0.3g/L, Sodium gluconate 15g/L, time 60 min, pH 9, temperature 900C.

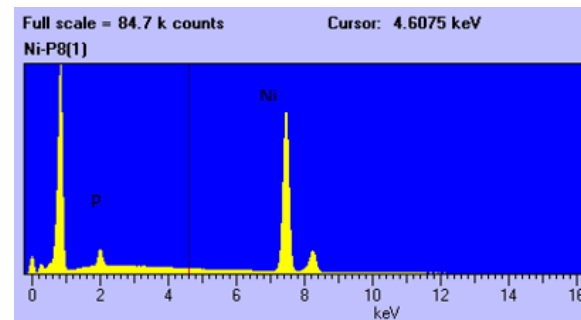


**Figure 4.** EDX chart of Ni88%-P12% alloy obtained from a bath containing NiSO<sub>4</sub>.6H<sub>2</sub>O 25g/L, Sodium hypophosphite 15g/L, Am. Sulfate 15 g/L, sodium dodecyl sulfate 0.1g/L, Succinic acid 0.3g/L, Sodium gluconate 15g/L, time 60 min, pH 9, temperature 900C.

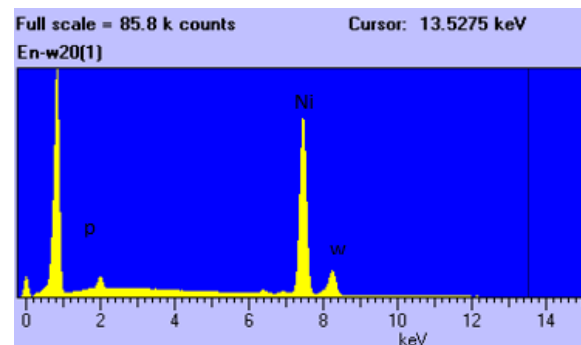


**Figure 5.** EDX chart of Ni91%-P3%-W6% alloy obtained from a bath containing NiSO<sub>4</sub>.6H<sub>2</sub>O 25g/L, Sodium hypophosphite 15g/L, sodium tungsten 5g/L, Am. Sulfate 15 g/L, sodium dodecyl

sulfate 0.1g/L, Succinic acid 0.3g/L, Sodium gluconate 15g/L, time 60 min, pH 9, temperature 900C.

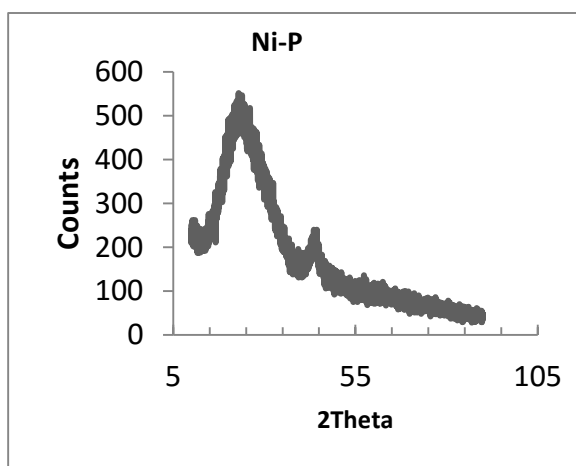


**Figure 6.** XRD chart of Ni-P alloy obtained from a bath containing NiSO<sub>4</sub>.6H<sub>2</sub>O 25g/L, Sodium hypophosphite 15g/L, Am. Sulfate 15 g/L, sodium dodecyl sulfate 0.1g/L, Succinic acid 0.3g/L, Sodium gluconate 15g/L, time 60 min, pH 9, temperature 900C.

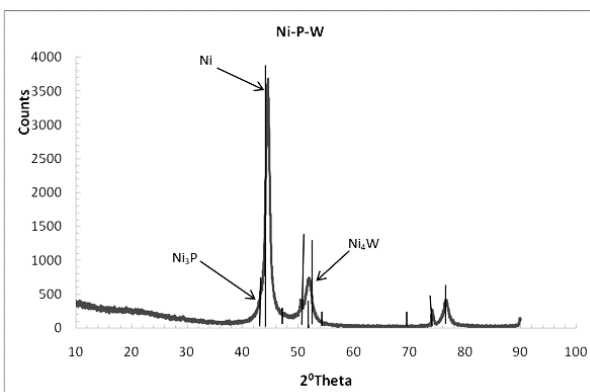


**Figure 7.** XRD chart of Ni<sub>91</sub>-P<sub>3</sub>-W<sub>6</sub> alloy obtained from a bath containing NiSO<sub>4</sub>.6H<sub>2</sub>O 25g/L, Sodium hypophosphite 15g/L, sodium tungsten 5g/L, Am. Sulfate 15 g/L, sodium dodecyl sulfate 0.1g/L, Succinic acid 0.3g/L, Sodium gluconate 15g/L, time 60 min, pH 9, temperature 900C.

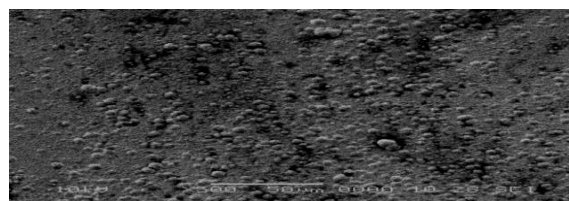


**Figure 8.** SEM of Ni-P alloy obtained from a bath containing NiSO<sub>4</sub>.6H<sub>2</sub>O 25g/L, Sodium hypophosphite 15g/L, Am. Sulfate 15 g/L, sodium dodecyl sulfate 0.1g/L, Succinic acid 0.3g/L, Sodium gluconate 15g/L, time 60 min, pH 9, temperature 900C.

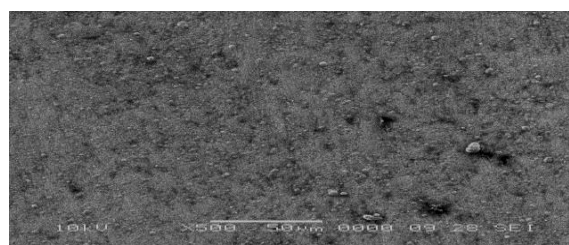


**Figure 9.** SEM of Ni<sub>91</sub>-P<sub>3</sub>-W<sub>6</sub> alloy obtained from a bath containing NiSO<sub>4</sub>.6H<sub>2</sub>O 25g/L, Sodium hypophosphite 15g/L, sodium tungsten 5g/L, Am. Sulfate 15 g/L, sodium dodecyl sulfate 0.1g/L, Succinic acid 0.3g/L, Sodium gluconate 15g/L, time 60 min, pH 9, temperature 900C.

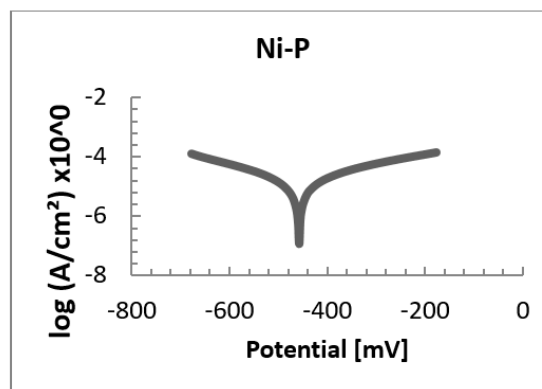


**Figure 11.** Corrosion behavior of Ni-P alloy obtained from a bath containing NiSO<sub>4</sub>.6H<sub>2</sub>O 25g/L, Sodium hypophosphite 15g/L, Am. Sulfate 15 g/L, sodium dodecyl sulfate 0.1g/L, Succinic acid 0.3g/L, Sodium gluconate 15g/L, time 60 min, pH 9, temperature 900C.

Table 4. Data of Potentiodynamic curve of Ni96-P4 alloy

E (i=0) mV	i corrosion $\mu\text{A}/\text{cm}^2$	Rp kohm.cm <sup>2</sup>	Beta a mV/ decade	Beta c mV/ decade	Corrosion Rate $\mu\text{m}/\text{Y}$
-225	0.2848	57.64	72.74	-89.7	3.296

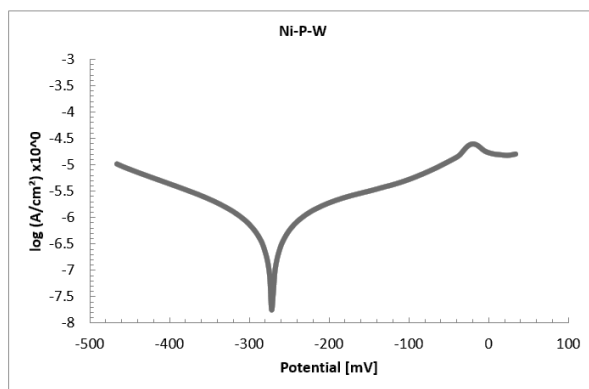


**Figure 12.** corrosion behavior of Ni94%-P2.5%-W3.5% alloy obtained from a bath containing NiSO<sub>4</sub>.6H<sub>2</sub>O 25g/L, Sodium hypophosphite 15g/L, sodium tungsten 5g/L, Am. Sulfate 15 g/L, sodium dodecyl sulfate 0.1g/L, Succinic acid 0.3g/L, Sodium gluconate 15g/L, time 60 min, pH 9, temperature 900C.

Table 5. Corrosion data of Ni94%-P2.5%-W3.5% alloy

E (i=0) mV	i corrosion $\mu\text{A}/\text{cm}^2$	Rp Kohm.cm <sup>2</sup>	Beta a mV/ decade	Beta c mV/ decade	Corrosion rate, $\mu\text{m}/\text{Y}$
-270.0	0.224	28.015	48.984	-55.530	2.620

#### 4. Conclusion:

At the present work Ni-P and Ni-P-W alloys were electroless plated from alkaline hypophosphite gluconate baths, the factors affected the plating conditions were studied. X-ray diffraction and SEM analysis shown that the morphological details, of as plated Ni-P coatings were greatly affected by the incorporation of W on the Ni-P matrix. Enhancement in hardness and corrosion resistance was also observed upon introducing of W on Ni-P coatings.

#### Corresponding Author:

M.S. Ali Eltoun, Ph.D.

Department of Chemistry, Faculty of Science, Sudan University of Science and Technology, Khartoum, Sudan.

E-mail: [abotteell74@gmail.com](mailto:abotteell74@gmail.com)

#### References

- 1- Aal, A. A., El-Sheikh, S. M., & Ahmed, Y. M. Z. (2009). Electrodeposited composite coating of Ni-W-P with nano-sized rod-and spherical-shaped SiC particles. *Materials Research Bulletin*, 44(1), 151-159.
- 2- Abd el Rehim, S. S., Sayyah, S. M., & El Deeb, M. M. (2000). Electroplating of tin from acidic gluconate baths. *Plating and surface finishing*, 87(9), 93-98.
- 3- Abd El Meguid, E. A., Abd El Rehim, S. S., & Moustafa, E. M. (1999). The electroplating of nickel from aqueous gluconate baths. *Transactions of the Institute of Metal Finishing*, 77, 188-191.
- 4- Balaraju, J. N., Anandan, C., & Rajam, K. S. (2006). Influence of codeposition of copper on the structure and morphology of electroless Ni-W-P alloys from sulphate-and chloride-based baths. *Surface and Coatings Technology*, 200(12), 3675-3681.
- 5- Balaraju, J. N., & Rajam, K. S. (2005). Electroless deposition of Ni-Cu-P, Ni-W-P and Ni-W-Cu-P alloys. *Surface and coatings technology*, 195(2), 154-161.
- 6- Balaraju, J. N., & Rajam, K. S. (2006). Influence of particle size on the microstructure, hardness and corrosion resistance of electroless Ni-P-Al<sub>2</sub>O<sub>3</sub> composite coatings. *Surface and Coatings Technology*, 200(12), 3933-3941.
- 7- Bangwei, Z., Wangyu, H., Xuanyuan, Q., Qinglong, Z., Heng, Z., & Zhaosheng, T. (1996). Preparation, formation and corrosion for Ni-WP amorphous alloys by electroless plating. *Transactions of the Institute of Metal Finishing*, 74, 69-71.
- 8- Brenner, A. (1963), Electrodeposition of Alloys. Principle and practice, *Academic Press*, New York, pp 345.
- 9- de Hazan, Y., Werner, D., Z'graggen, M., Groteklaes, M., & Graule, T. (2008). Homogeneous Ni-P/Al<sub>2</sub>O<sub>3</sub> nanocomposite coatings from stable dispersions in electroless nickel baths. *Journal of colloid and interface science*, 328(1), 103-109.
- 10- Du, N., & Pritzker, M. (2003). Investigation of electroless plating of Ni-W-P alloy films. *Journal of applied electrochemistry*, 33(11), 1001-1009.
- 11- El Rehim, S. A., Sayyah, S. M., & El Deeb, M. M. (2000). Electroplating of copper films on steel substrates from acidic gluconate baths. *Applied Surface Science*, 165(4), 249-254.

- 12- Hamdy, A. S., Shoeib, M. A., Hady, H., & Salam, O. A. (2008). Electroless deposition of ternary Ni-P alloy coatings containing tungsten or nano-scattered alumina composite on steel. *Journal of applied electrochemistry*, 38(3), 385-394.
- 13- Hu, Y. J., Wang, T. X., Meng, J. L., & Rao, Q. Y. (2006). Structure and phase transformation behaviour of electroless Ni-W-P on aluminium alloy. *Surface and Coatings Technology*, 201(3), 988-992.
- 14- Jin, Y., Fan, J., Mou, K., Wang, X., Ding, Q., Li, Y., & Liu, C. (2010). Structural and phase transformation behaviour of electroless Ni-W-Cr-P alloy coatings on stainless steel. *Inorganic Materials*, 46(6), 631-638.
- 15- Lu, G., & Zangari, G. (2002). Corrosion resistance of ternary Ni-P based alloys in sulfuric acid solutions. *Electrochimica Acta*, 47(18), 2969-2979.
- 16- Pearlstein, F., Weightman, R., & Wick, R. (1963). Nickel-Tungsten electroless deposition. *Metal Finishing*, 61, 77.
- 17- Rashwan, S. M., Mohammed, A. E., El Wahaab, S. A., & Kamel, M. M. (2000). Mansoura Science Bulletin A. *Chemistry*, 27, 121.
- 18- Szczygieł, B., & Turkiewicz, A. (2008). The effect of suspension bath composition on the composition, topography and structure of electrolessly deposited composite four-component Ni-W-P-ZrO<sub>2</sub> coatings. *Applied Surface Science*, 254(22), 7410-7416.
- 19- Tien, S. K., Duh, J. G., & Chen, Y. I. (2004). Structure, thermal stability and mechanical properties of electroless Ni-P-W alloy coatings during cycle test. *Surface and Coatings Technology*, 177, 532-536.

Received January 13, 2016; revised January 15, 2016; accepted January 15, 2016; published online February 1, 2016.